

THE RESEARCH ON QUALITY INSPECTION OF LAND COVER CLASSIFICATION BASED ON LIDAR

Shen jing, Han wenli, Zhang libo, Li hai*, Lyu linbing

(National Quality Inspection and Testing Center for Surveying and Mapping Products, Beijing 100830, China)

Commission IV, WG IV/III

KEY WORDS: Land Cover Classification, Quality Inspection, LiDAR, Filter, Morphology.

ABSTRACT:

Aiming at the quality inspection of land cover classification in natural resources investigation and monitoring, a method and process for quickly inspecting land cover misclassification and omission by using airborne Lidar data are proposed. Firstly, the ground objects are separated from laser feet points by post-processing such as gross error elimination, multi echo analysis and filtering of airborne Lidar data. Secondly, the elevation information is used to distinguish the easily confused ground objects with the similar spectral characteristics, such as forest land and shrub grass, the building area and road, high-rise houses and low-rise houses. Finally, overlay and compare the classified laser feet points with land cover achieving the misclassification. Experiments shows the effectiveness of this method, improve the quality inspection efficiency of land cover classification results, reduce the workload of field data collection, and improve the accuracy of quality inspection.

1. INTRODUCTION

Data product verification is an important basic work of remote sensing land cover mapping and analysis application at home and abroad (CHEN Jun, 2018). The accurate characterization of land cover classification is very important for the application, such as ecological environment monitoring, land resource management, land spatial planning, and natural resource investigation and monitoring. The feature extraction of natural resource based on remote sensing images is the most basic, widely used, but most technically difficult work in investigation and monitoring (Zhang Jixian, 2021). At present, the widely used data source for land cover classification is satellite remote sensing image that has become the main data source for land cover because of its fast data acquisition and wide coverage. However, it is difficult to distinguish between ground objects with similar spectral characteristics and different elevation information (lahat et al., 2015), such as roofs and roads, trees and shrubs, high-rise houses and low-rise houses, etc. In addition, the national geographic situation monitoring project conducted statistics on 1311 samples collected from the geographic situation survey dataset, and found that there were 94 groups of easily mixed in the land cover, 36 groups of quality inspection within the first class and 58 groups of types across the first class (Gao Zhihong, 2015). It can be seen that due to the same object with different spectrum and different object with the same spectrum of the optical imaging principle, the classification errors and omissions of the land cover classification have an impact on the use. In the quality inspection link, due to the limited reference data, the inspection mainly depends on the manual comparison with the production data source, and the suspected land type spots can not be determined. Therefore, it is necessary to find a more suitable quality inspection reference data source according to the characteristics of optical images and the characteristics of confused types of existing land cover classification. Unlike optical images, Lidar is an active remote sensing technology. Its data has more accurate three-dimensional spatial information (Zhang et al., 2013), which can

classify ground objects by height. In addition, laser has certain penetration ability, and can obtain high-precision terrain surface data of vegetation covered areas (Wu Huayi, 2006). This paper presents a detection process and method of easily confused ground objects in classification of land cover based on airborne Lidar data, which improves the efficiency and accuracy of land cover quality inspection.

2. THE FRAMEWORK OF OUR PROPOSED METHOD

The quality inspection process of land cover based on airborne Lidar data is shown in Figure 1. It mainly includes gross error elimination, multi echo analysis, filtering, comparison and verification, etc. In detail Firstly, the gross error of the LIDAR point cloud data is eliminated, and then the LIDAR point cloud is filtered by using the multi echo information and morphological method to obtain the separated ground points and non-ground points. The buildings in the non-ground points are separated from the vegetation by using the multi echo information, and then the high-rise buildings in the buildings are separated from the low buildings by using the elevation information and the woodland are separated from the shrub and other vegetation. Finally, the classification results obtained by Lidar are overlaid with the landcover to quickly find the suspected misclassification areas.

* corresponding author; Email: 29292638@qq.com

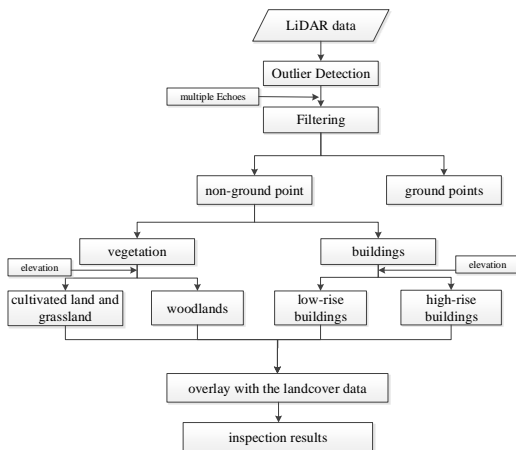


Figure 1. The flowchart of the quality inspection of land cover with LiDAR

2.1 K-D Tree

A LiDAR point cloud dataset is composed of a great number of discrete 3D points. K-d trees are a useful data structure for several applications, such as searches involving a multidimensional search key (e.g. range searches and nearest neighbor searches). The k-d tree is a binary tree in which every node is a k-dimensional point. Every non-leaf node can be thought of as implicitly generating a splitting hyperplane that divides the space into two parts, known as subspaces.

In this paper, KD tree is selected for coarse error removal. The specific process is as follows: build a 3D KD tree from LIDAR point cloud data, calculate the average value of laser foot elevation in each block, give a search radius R (more than twice the ground resolution) for laser feet below the average value, and count the number of laser feet with the laser foot as the circle center and the radius as R. If the number of laser foot points is less than the given threshold, it is considered to be a very low coarse defect.

2.2 Analyzing the Echo Information

Currently, the multi-pulse airborne LiDAR system is capable of recording both singular return and multiple returns, and the difference between the above two types of echoes is that whether a laser pulse would occur multiple reflections. In this paper, for multiple echoes, the first one received is called the first return, the last one received is called the last return, and the intermediate ones between the first return and the last return are called intermediate returns.

Existing research suggests that the number of echoes can reflect the type of a target, as shown in Figure 2. The echo information analysis shows that the last returns and singular returns may come from the ground surfaces or non-ground objects; the first returns and intermediate returns are sure to come from the non-ground objects. Thus, the proportion of the first returns and intermediate returns in each cluster of point clouds will be a good feature to distinguish non-ground objects from ground objects.

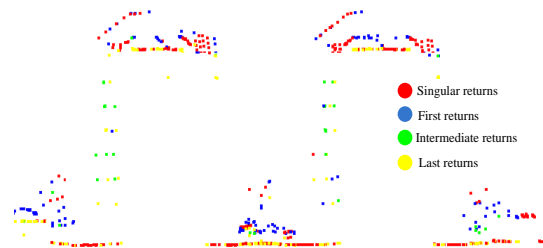


Figure 2. Relationship between types of echoes and types of objects in urban areas (Xiangguo Lin, 2011)

2.3 Filtering

The basic operation of morphology is generally carried out in the grid. Therefore, this algorithm records the elevation value of the echo retained in step 2.2 into a grid image. If several laser foot points fall into a grid, record the point with the lowest elevation value into the grid. When the point spacing of the laser foot points is greater than the spatial resolution of the image, there are no values in some cell networks. In this case, it can be filled with the nearest grid values with elevation values. However, due to the original laser point cloud data, there is often a lack of data in a large area, such as water area. If the nearest laser foot point filling method is used, there will be multiple elevation values on the same water surface. In this paper, the Euclidean distance transform is used to fill all the areas without data, then the data missing area is detected, and the data missing area is filled with the lowest elevation value around it.

The principle of morphological reconstruction is as follows. Morphological reconstruction is one of the important components of morphology (Soille P, 2008), which is mainly based on geodesic transformation. Geodesic transformation has been widely used in gray image restoration and reconstruction. Its basic operations include geodesic expansion and geodesic corrosion (Lantuejoul C, 1984). Geodesic expansion involves two images: marker image and mask image. The two images have the same size and the same domain; And the value of each pixel of the mask image must be greater than or equal to the value of the corresponding pixel at the same position of the marked image. The expansion process is: the basic isotropic structural elements are used to expand the marked image, but the resulting image must be kept under the mask image, that is, the mask image plays a role in limiting the expansion and spread of the marked image. It is assumed f as a marker image, g as a mask image, and $f \leq g$. The geodesic expansion of the marked image f relative to the mask image g is expressed as $\delta_g^{(1)}(f)$ when the scale is 1, then the geodesic expansion is defined as the point by point minimum $\delta^{(1)}$ between the basic expansion operations of the mask image and the marked image:

$$\delta_g^{(1)}(f) = \delta^{(1)}(f) \wedge g \quad (1)$$

Geodesic corrosion is the dual transformation of the complement of the corresponding set of geodesic expansion, which is recorded as:

$$\delta_g^{(1)}(f) = \delta^{(1)}(f) \wedge g = \varepsilon^{(1)}(f) \vee g \quad (2)$$

The geodesic expansion or geodesic corrosion transformation of gray image will always converge after a certain number of cycles, until the expansion or contraction of the marked image is

completely prevented by the submerged image; At this time, the value of any pixel of the marked image will not change again. The morphological reconstruction of mask image from marker image is based on this principle. The expansion reconstruction of the mask image g ($f \leq g$) from the marker image f is expressed as $R_g^\delta(f)$, which is defined as the geodesic expansion f relative to g until it is stable:

$$R_g^\delta(f) = \delta_g^{(i)}(f) \quad (3)$$

Where i is the number of cycles $\delta_g^{(i)}(f) = \delta_g^{(i+1)}(f)$, as shown in Figure 3. Similarly, the corrosion reconstruction of the mask image g from the marker image f is expressed as $R_g^\varepsilon(f)$, which is defined as the geodesic corrosion f relative to g until it is stable:

$$R_g^\varepsilon(f) = \varepsilon_g^{(i)}(f) \quad (4)$$

Where i is the number of cycles $\varepsilon_g^{(i)}(f) = \varepsilon_g^{(i+1)}(f)$.

In this paper, geodesic expansion operation is used to filter Lidar data. The principle is shown in Figure 3. Record the DSM data obtained by feet point interpolation as a mask image I ; A new image is obtained by subtracting a positive number h (which is the average height difference between the ground object and the ground surface. Its value depends on the actual situation of the area) from the value of each pixel of the image I . It is recorded as a marker image M . Then, the labeled image M is expanded and reconstructed with a mask I . Finally, if the image I obtained by subtraction reconstruction I' is used, the points with the difference greater than 0 are usually non-ground points.

To extract the ground points from the LiDAR data, six major steps are involved. Lidar data are divided into ground points and non-ground points, which can assist in the inspection of roads and buildings that are difficult to distinguish in optical remote sensing images. The ground laser foot points are extracted from the laser feet points data after gross error elimination and multi echo analysis, and they are rasterized and missing areas filled. Finally, the rasterized images are morphologically filtered to obtain ground points and non-ground points. The specific process is as follows:

(1) Generate raster image

The density of Lidar point cloud data is set to be d (number of laser feet per square meter), and the resolution of the image to be generated is C (unit: meter). Firstly, the image of the point cloud is generated according to the above nearest neighbor interpolation rules. Then, a mask image of the same size is generated. The grid value of the laser foot is 1, otherwise it is 0.

(2) The location and filling of the no-data area

The outer distance Euclidean distance transformation is carried out on the mask image. In the transformation process, the standard to distinguish between entity and non entity is: the pixel with value of 1 is entity, and the pixel with value of 0 is non entity. Binarize the mask image obtained by distance transformation. If the value of the pixel is greater than r , the value is 1; Otherwise, it is 0. The region with a median value of 1 in the mask image is a cavity region. For areas with missing data, fill with the

minimum value of elevation value in the grid around the area. r is the average number of grids between two valuable grids, and its generation rule is:

$$r = \left(\frac{1}{d}\right)^{0.5} \cdot \frac{1}{c} \quad (5)$$

(3) Morphological reconstruction to obtain non-ground points

In this paper, geodesic expansion operation is used to filter the Lidar data. The principle is shown in Figure 3.

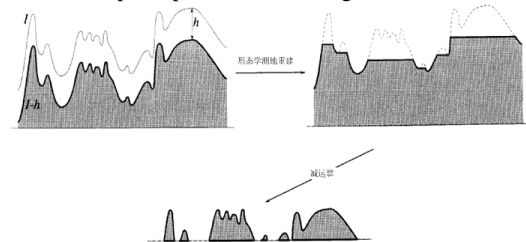


Figure 3. Figure of data filtering based on morphological reconstruction (Cited from literature Lantuejoul C,1984)

Label the DSM data obtained by point cloud data interpolation as a mask image; A new image labeled as marker image M is obtained by subtracting a positive number from the value of each pixel of the image I (h is the average height difference between the ground object and the non-ground object. Its value depends on the actual situation of the region, and the value in this paper is between 3 and 10m). Then, the marker image M is expanded and reconstructed masked with I . Finally, subtract the image I' obtained by reconstruction from image I , and then the points with a difference greater than 0 are usually non-ground points. The detailed process is as follows:

- ① Taking the image obtained in step (1) as a mask image I , subtracting a positive number from the each pixel of image I to obtain a marker image M ;
- ② The morphological reconstruction operation is carried out with formulas (1) and (3)(seen in literature SHEN Jing,2011), and the reconstructed image is labeled as I' .
- ③ The normalized digital surface model (NDSM) is obtained by the formula(6)(seen in literature SHEN Jing,2011).
- ④ Analyze the regional connectivity and detect the regions with non-zero value in NDSM image;
- ⑤ For any region detected in ④, if the number of pixels with the corresponding edge gradient intensity value greater than 0.5 in the boundary pixels of the region accounts for more than 90% of the total number of boundaries, it is determined that the region is a non-ground region. Then fill the region with the minimum value of the elevation value in the grid around the region, and exclude the region from the mask image I ; Otherwise, the corresponding pixel value of the mask image I is assigned;
- ⑥ Restart the operation from ① until no pixel is judged as a non-ground point.

(4) Recovery and category determination of laser foot points

If the difference between the elevation of the laser foot point and the corresponding grid point is 0, it is a ground point; Otherwise, it is a non-ground point.

2.4 Classification and Extraction of Non-ground Points

The DEM data is subtracted from the DSM data to obtain the normalized digital surface model. On the basis, vegetation and buildings are separated in the normalized digital surface model.

(1) Building extraction

Firstly, set the minimum area value, search all planes in the point cloud data according to the value, calculate the area of each plane, eliminate the areas less than the set minimum value, then set the minimum height threshold, and filter out the planes higher than the threshold by near ground filtering as the extracted building area. In addition, considering the influence of noise during data acquisition, the plane tolerance parameter is added when searching the plane. By default, the point cloud data within this tolerance range are in one plane.

(2) Vegetation extraction

In the normalized digital surface model, the building area is eliminated, and the elevation information is used to separate trees from shrubs and grass.

2.5 Comparison and Verification

The trees, shrubs, roads, high-rise houses and low-rise houses classified by Lidar data are colored in layers and overlaid with the land cover by category display map to find the possible errors and omissions of the classification of land cover.

3. EXPERIMENT

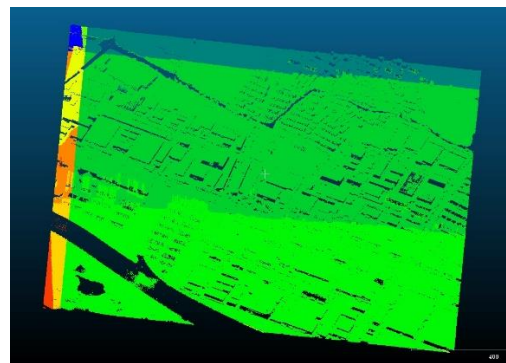
The LiDAR data is processed with Point Cloud Catalyst by human-computer interaction. The hardware we used is a ThinkPad workstation W540, with Intel (R)Core(TM)i7-4700MQ CPU 2.4GHz and 8-GB RAM.

3.1 Testing Datasets

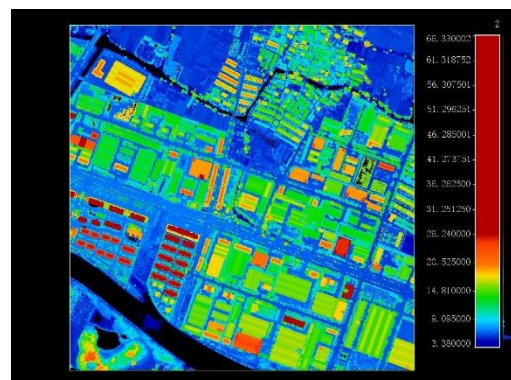
One point cloud dataset is used to test our approach. The data is over some town of China with 1000m width and 1000m length, as shown in Figure 4(a). The dataset was recorded with the FLI-MAP 400 system with 7points/m², and maximum number of returns of per pulse reaches to 4. The ground surface is very flat. There are some trees surrounded by shrub, lots of low-rise buildings and some high-rise buildings in this scene seen in the Figure 4(a).



(a) Image of the test dataset

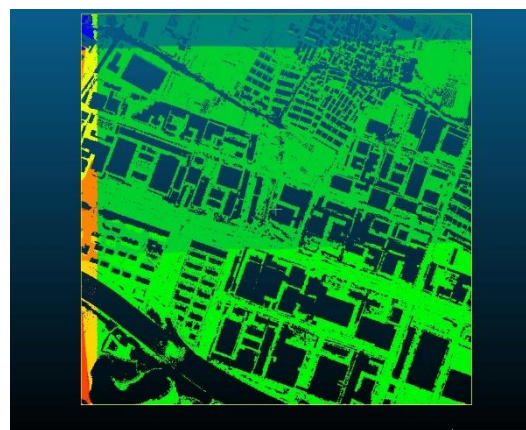


(b) Perspective view of unclassified point cloud

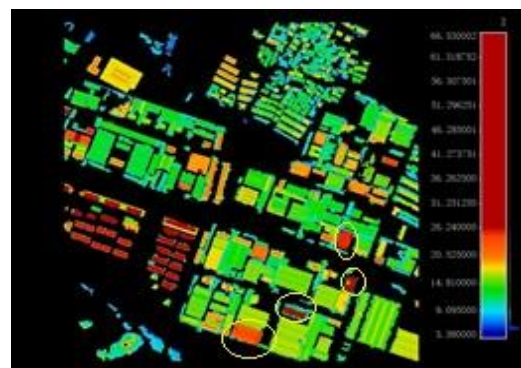


(c) Perspective view of classified point cloud colored by elevation value

Figure 4. Datasets for the test



(a)Figure of the ground point

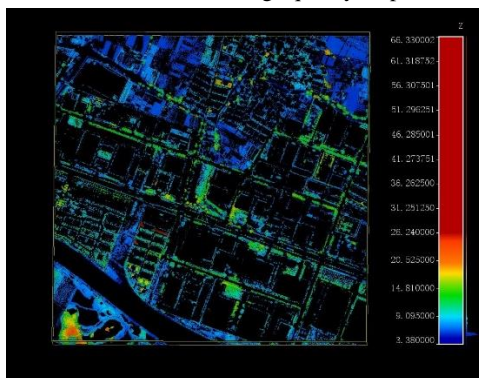


(b) Figure of the buildings colored by elevation value

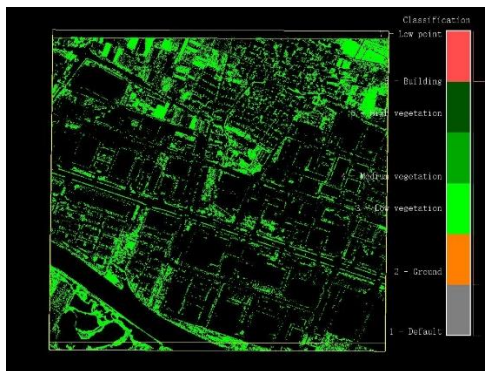


(c) Figure of the buildings that was misclassified to low-rise buildings checked by the Lidar points

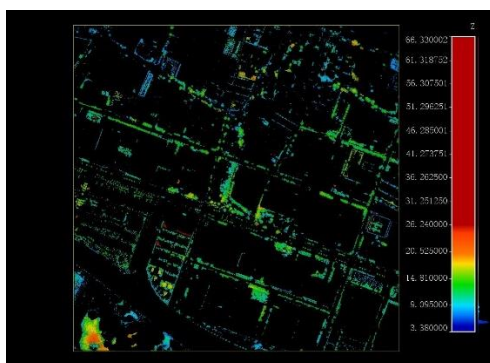
Figure 5. Results of the buildings quality inspection



(a) Figure of the vegetation colored by elevation value



(a) Figure of submerge vegetation



(b) Figure of woodland



(c) Figure of omission of the woodland

Figure 6. Results of the vegetables quality inspection

3.2 Results and Discussion

The experimental results are showed in Figure 5. and Figure 6. respectively. Visual observation tells us that our proposed method works well on the testing dataset. In detail, it is capable of distinguishing most of building points and tree points. The test results show that some high-rise buildings surrounded by low-rise buildings are difficult to check from optical remote sensing image, but it is easy to achieve by the Lidar data with the difference of elevation as shown in Figure 5(b). and Figure 5(c). And the woodland distinguished from the other vegetation is also achieved as shown in Figure 6. Then the woodland with higher elevation as shown in Figure 6(c). overlay with the woodland colored by green as shown in Figure 6(d). to check misclassification and omission. But there are also some misclassified points. Obviously, some trees points are mistakenly classified into the building points in the scene. Although there was some misclassification in the automatic classification of airborne Lidar data, this error can be ignored compared with the traditional inefficient field measurement, because the method significantly shortens the time for verifying the classification of land cover. In addition some classification result from Lidar cannot be interpreted and checked through the optical remote sensing image. Most of all, the approach increases efficiency and shortens the time of quality inspection. Overall, our method obtains a desired accuracy in point cloud classification and the results of the inspection are satisfied.

4. CONCLUSION

Rapid quality inspection of land cover is the key to ensure high-quality management of natural resources. The traditional manual inspection has low efficiency, poor reliability, difficult to ensure quality, labor intensive and time consuming. Based on this, this paper introduces a fast land cover quality inspection method based on airborne Lidar data. The algorithm first eliminates the very low gross error, then extracts and retains the single echo and the last echo, interpolates the retained laser feet points into the image, and gradually removes the ground area through iterative morphological reconstruction operation. In the iterative process, the gradient intensity is used as the criterion to distinguish the non-ground area from the ground area, and the LIDAR point cloud data recovery and category definition are carried out through height difference. Finally, the classified feet points are superimposed with the land cover to find the misclassification and omission. The experimental results show that the method has

advantage to achieve the quick and accurate inspection results. This shows that the algorithm in this paper has better reliability and practicability. At present, the reference data source cited in this paper is Lidar. The next research will focus on the cross validation of multiple reference data sources to achieve the quick land cover quality inspection.

Lantuejoul C, Maisonneuve F. Geodesic Methods in Quantitative Image Analysis [J]. *Pattern Recognition*, 1984, 17: 117–187

ACKNOWLEDGEMENTS

This research was funded by Science and Technology Project of Ministry of Natural Resources of China: Support Service System for Natural Resources Satellite Remote Sensing Business (grant No. 1211340000019 0002).

REFERENCES

CHEN Jun, CHEN Fei, WU Hao, CHEN Lijun, HAN Gang. Internet+ Land Cover Validation: Methodology and Practice[J]. *Geomatics and Information Science of Wuhan University*, 2018, 43(12): 2225-2232.

ZHANG Jixian, LI Haitao, GU Haiyan, ZHANG He, YANG Yi, TAN Xiangrui, LI Miao, SHEN Jing. Study on man-machine collaborative intelligent extraction for natural resource features[J]. *Acta Geodaetica et Cartographica Sinica*, 2021, 50(8): 1023-1032.

Lahat D, Adali T and Jutten C. 2015. Multimodal data fusion: an overview of methods, challenges, and prospects. *Proceedings of the IEEE*, 103(9): 1449–1477

GAO Zhihong, ZHOU Xu, CHENG Tao. Statistical Analysis of the Confusing Land Cover Types in China Geography Census[J]. *bulletin of surveying and mapping*, 2015, 0(6): 32-34..

ZHANG Jixian, LIN Xiangguo, LIANG Xinlian. Advances and Prospects of Information Extraction from Point Clouds[J]. *Acta Geodaetica et Cartographica Sinica*, 2017, 46(10): 1460-1469.

SHEN Jing, LIU Jiping, LIN Xiangguo. Airborne LiDAR Data Filtering by Morphological Reconstruction Method[J]. *Geomatics and Information Science of Wuhan University*, 2011, 36(2): 167-170.

Jing S , Liu J , Rong Z , et al. A Kd-Tree-Based Outlier Detection Method for Airborne LiDAR Point Clouds. *IEEE*, 2011.

J. L. Silván-Cárdenas and L. Wang, “A multi-resolution approach for filtering LiDAR altimetry data,” *ISPRS Journal of Photogrammetry and Remote Sensing*, vol. 61, pp. 11-22, 2006.

Lin X , Zhang J , Jing S . Object-Based Classification of Airborne LiDAR Point Clouds with Multiple Echoes. *IEEE*, 2011.

Lantuejoul C, Maisonneuve F. Geodesic Methods in Quantitative Image Analysis [J]. *Pattern Recognition*, 1984, 17: 117–187.

M. G. Vosselman, B. G. H. Gorte, G. Sithole and T. Rabbani, “Recognizing structure in laser scanner point clouds,” *International Archives of the Photogrammetry, Remote Sensing and Spatial Information Sciences*, vol. 36, pp. 33-38, 2004.

J. L. Silván-Cárdenas and L. Wang, “A multi-resolution approach for filtering LiDAR altimetry data,” *ISPRS Journal of Photogrammetry and Remote Sensing*, vol. 61, pp. 11-22, 2006.

Soille P. *Morphological Image Analysis: Principles and Applications* [M]. Berlin/Heidelberg/New York: Springer-Verlag, 2008